

# Loss of human Greatwall results in G2 arrest and multiple mitotic defects due to deregulation of the cyclin B-Cdc2/PP2A balance

Andrew Burgess, Suzanne Vigneron, Estelle Brioudes, Jean-Claude Labbé, Thierry Lorca<sup>1,2</sup>, and Anna Castro<sup>1,2</sup>

Universités Montpellier 2 et 1, Centre de Recherche de Biochimie Macromoléculaire, Centre National de la Recherche Scientifique UMR 5237, 34293 Montpellier Cedex 5, France

Edited by Tim Hunt, Cancer Research UK, South Mimms, United Kingdom, and approved April 21, 2010 (received for review December 9, 2009)

Here we show that the functional human ortholog of Greatwall protein kinase (Gwl) is the microtubule-associated serine/threonine kinase-like protein, MAST-L. This kinase promotes mitotic entry and maintenance in human cells by inhibiting protein phosphatase 2A (PP2A), a phosphatase that dephosphorylates cyclin B-Cdc2 substrates. The complete depletion of Gwl by siRNA arrests human cells in G2. When the levels of this kinase are only partially depleted, however, cells enter into mitosis with multiple defects and fail to inactivate the spindle assembly checkpoint (SAC). The ability of cells to remain arrested in mitosis by the SAC appears to be directly proportional to the amount of Gwl remaining. Thus, when Gwl is only slightly reduced, cells arrest at prometaphase. More complete depletion correlates with the premature dephosphorylation of cyclin B-Cdc2 substrates, inactivation of the SAC, and subsequent exit from mitosis with severe cytokinesis defects. These phenotypes appear to be mediated by PP2A, as they could be rescued by either a double Gwl/PP2A knockdown or by the inhibition of this phosphatase with okadaic acid. These results suggest that the balance between cyclin B-Cdc2 and PP2A must be tightly regulated for correct mitotic entry and exit and that Gwl is crucial for mediating this regulation in somatic human cells.

spindle assembly checkpoint | cell cycle | phosphatase | kinase | slippage

In eukaryotic cells, the mitotic state is maintained by the mitotic kinase cyclin B-Cdc2. Historically, mitotic entry and exit was thought to be the direct consequence of cyclin B-Cdc2 activation and inactivation, respectively (1). Recent results have expanded this model to include phosphatases (2). Specifically, recent evidence indicates that protein phosphatase 2A (PP2A) is responsible for dephosphorylation of cyclin B-Cdc2 substrates and that the regulation of this dephosphorylation is required in mitotic entry and exit (3). This finding suggests a previously unexplored model in which the balance between cyclin B-Cdc2 and PP2A controls mitotic entry and exit. Thus, during G2 PP2A activity is high and cyclin B-Cdc2 activity low, thereby preventing phosphorylation of mitotic substrates, whereas at mitotic entry the balance flips, allowing entry into mitosis. The mechanisms controlling cyclin B-Cdc2 activity have been largely described (4). Briefly, cyclin B-Cdc2 is inhibited during G2 by inhibitory phosphorylations on threonine 14 and tyrosine 15 by Wee1 and Myt1 kinases. Upon mitotic entry, these are removed by the Cdc25 phosphatase (4). Finally, at mitotic exit cyclin B-Cdc2 is inhibited by the ubiquitin-dependent degradation of its regulatory subunit cyclin B (5). Unlike cyclin B-Cdc2 regulation, very little is known about the mechanisms controlling PP2A activity during mitosis, and therefore our understanding of G2 and mitosis is incomplete.

Recently, Greatwall (Gwl), a unique critical mitotic regulator, has been discovered in *Drosophila* (6, 7). It is a member of the AGC family of serine/threonine kinases that phosphorylates substrates on S/T residues encircled by basic amino acids (7). Work done in *Xenopus* egg extracts suggested that Gwl promoted mitotic entry by controlling the auto-amplification loop of cyclin B/Cdc2 (8, 9). However, it has been recently demonstrated that the main role of this kinase is not the regulation of cyclin B-Cdc2 activity but the inhibition of PP2A, the phosphatase that de-phosphorylates cyclin B-Cdc2 substrates (10, 11).

Despite the critical roles of Gwl in mitosis, the functional human ortholog of this kinase is currently unknown. The human protein with the closest homology to *Drosophila* and *Xenopus* Gwl is the microtubule-associated serine/threonine kinase-like (MAST-L) (50.2 and 65.7% of sequence homology, respectively) (Fig. S1). In addition to the high homology of MAST-L with the other members of the Gwl family, it also contains a very long T-loop (>500 amino acids) that separates the kinase subdomains VII and VIII, a particular feature exclusive to Gwl kinases. In contrast, although MAST-L was first classified as a member of the MAST family, it contains very little homology to any of the MAST kinases. All of the members of the MAST family are large enzymes (1,309–2,444 amino acids) with a short T-loop (31 amino acids for MAST1), and contain a PDZ domain in the C terminus. However, MAST-L has minimal homology to MAST proteins (10.4% with MAST1) and no PDZ domain, suggesting that it is not a true member of the MAST family.

Very little is known about the role of MAST-L in human cells, with only two publications to date. Both of these publications focus on the role of MAST-L in autosomal-dominant thrombocytopenia, showing that a single-point mutation (E167D) in the N-terminal kinase domain correlates with this syndrome (12), and transient knockdown in zebrafish results in a reduction of circulating thrombocytes (13).

In the present study, we verified that MAST-L is the functional human ortholog of Gwl. Using siRNA knockdown of hGwl, we show in human cells that this kinase mediates mitotic entry and maintains the mitotic state by inhibiting PP2A, and thus maintains the correct equilibrium between cyclin B-Cdc2 and PP2A.

## Results

**MAST-L Is the Functional Human Homolog of *Xenopus* Greatwall.** To analyze the role of Gwl in human cells, we cloned the closest related human protein to the *Drosophila* and *Xenopus* Greatwall, MAST-L (Fig. S1). Our previous results demonstrated that the depletion of Gwl from mitotic egg extracts induced the loss of the mitotic state. To check whether MAST-L corresponds to the Gwl ortholog, we translated MAST-L in M-phase frog egg extracts (CSF extracts) and tested its capacity to rescue the loss of endogenous Gwl. The expression, at endogenous levels, of WT MAST-L in these CSF extracts completely rescued the mitotic state (Fig. S2A). However, expression of a kinase-dead mutant of MAST-L failed to rescue, indicating that MAST-L is the functional orthologue of Gwl. Thus, from now on, it will be referred to as “human Greatwall” (hGwl) in this article.

Author contributions: A.B., T.L., and A.C. designed research; A.B., S.V., E.B., and J.-C.L. performed research; A.B., T.L., and A.C. analyzed data; and A.C. wrote the paper.

The authors declare no conflict of interest.

This article is a PNAS Direct Submission.

See Commentary on page 12409.

<sup>1</sup>T.L. and A.C. contributed equally to this work.

<sup>2</sup>To whom correspondence may be addressed. E-mail: anna.castro@crbm.cnrs.fr or thierry.lorca@crbm.cnrs.fr.

This article contains supporting information online at [www.pnas.org/lookup/suppl/doi:10.1073/pnas.0914191107/-DCSupplemental](http://www.pnas.org/lookup/suppl/doi:10.1073/pnas.0914191107/-DCSupplemental).

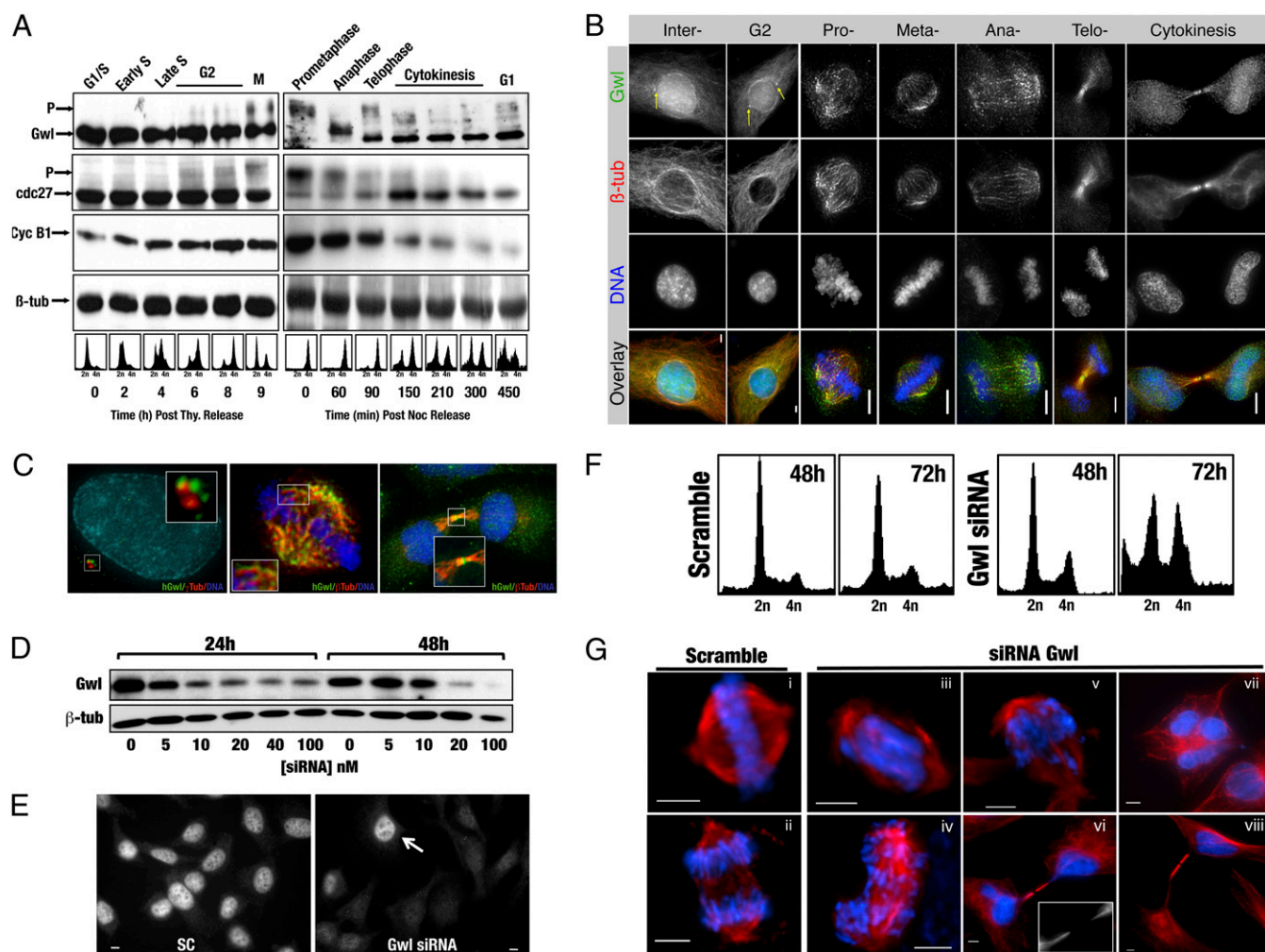


**Fig. 1.** hGwl siRNA knockdown induces multiple mitotic defects. (A) HeLa cells were synchronized by either thymidine (Thy) or nocodazole (Noc) shake-off and released into fresh media. Samples were collected at the indicated times and processed for Western blot. Cell synchrony was confirmed by FACS. (B) HeLa cells were probed with anti-hGwl (green), anti- $\beta$ -tubulin (red), and DAPI (DNA, blue). The maximum projections from 0.3- $\mu$ m Z-sections are shown. Yellow arrows indicate the centrosomal localization of hGwl. (Scale bars, 5  $\mu$ m.) (C) Enlargements of HeLa cells treated as per B. Cells were counterstained with  $\gamma$ - (interphase, red) or  $\beta$ -tubulin (mitotic, cytokinesis, red), hGwl (green), and DNA (blue). (D) Asynchronous HeLa cells were transfected with the indicated amounts of hGwl siRNA for 24 h and harvested immediately (24 h) or 1 d later (48 h). The levels of hGwl were analyzed by Western blot. (E) Asynchronous HeLa cells were transfected with 50 nM of siRNA and analyzed by immunofluorescence with anti-hGwl antibodies. Arrow indicates a nontransfected cell. (F) HeLa cells were treated as per D with either 50 nM of Scramble or hGwl siRNA and analyzed by FACS. (G) Asynchronous HeLa cells treated as in D were analyzed by immunofluorescence. For  $\beta$ -tubulin (red) and DAPI (DNA, blue). (Scale bars, 5  $\mu$ m.)

We next analyzed by Western blot the expression of the endogenous human protein in HeLa cells. Our antibodies clearly recognized and specifically immunoprecipitated a band around 110 kDa, the expected molecular weight of hGwl (Fig. S2B). The levels of hGwl appeared to be constant throughout the cell cycle (Fig. 1A and Fig. S2C and D). However, a lower electrophoretic mobility of this protein appeared as cells entered mitosis, was maximal in prometaphase, and disappeared by anaphase (Fig. 1A). This lower mobility was induced by phosphorylation as  $\lambda$ -Phosphatase treatment reversed the shift (Fig. S2E).

Previously in *Drosophila*, Gwl was identified as a nuclear protein (7). However, although hGwl is mostly present in the nucleus of interphase human cells, we also noted a consistent partial localization in the cytoplasm and at the centrosomes during G1, S, and G2 phases (Fig. 1B). The centrosomal hGwl appeared to surround  $\gamma$ -tubulin, indicating that hGwl is localized around the pericentriolar material (Fig. 1C). As cells entered mitosis, hGwl concentrated at the poles of the spindle and emanated out along the microtubule spindle fibers (Fig. 1B and C). At anaphase, the protein started to leave the mitotic spindle, eventually becoming more diffuse in the cytoplasm. Finally, from telophase to cytokinesis, once the nuclear membrane reformed, most of the hGwl

was localized in the nucleus, but a small fraction stayed at the cleavage furrow where it remained on the midzone microtubules, although occasionally it was also observed at the midbody (Fig. 1C). We detected a similar localization of this protein in U2OS cells and by using two different antibodies, one against the full-length protein and the other against the last 12 C-terminal amino acids of hGwl.

**hGwl Knockdown Promotes G2 Arrest and Mitotic Defects in HeLa Cells That Can Be Rescued by the Knockdown or the Inhibition of PP2A by Okadaic Acid.** It has been previously shown that depletion of Gwl in *Xenopus* egg extracts both prevents mitotic entry and promotes mitotic exit (8, 10, 11).

To investigate the role of hGwl in human cells, we induced its knockdown by siRNA in HeLa cells. The levels of hGwl decreased in a dose-dependent manner when increasing doses of the hGwl siRNA were used, with an almost complete knockdown of this protein after 48 h with a 100-nM dose of this siRNA, both by Western blot (Fig. 1D) and immunofluorescence (Fig. 1E).

We next analyzed if knockdown of hGwl in cells resulted in any alteration in mitotic entry or in the maintenance of the mi-

otic state. FACS, after a 48-h siRNA treatment of asynchronous cells, produced an accumulation (40%) of cells with a 4n DNA content and a notable increase of subdiploid cells, indicating that the knockdown of hGwl induced G2/M cell cycle-dependent defects and an increase in cell death (Fig. 1F).

Immunofluorescence analysis revealed that the accumulation of cells with 4n DNA content was not primarily because of an increase in the mitotic index (6.9% of mitotic cells from 40% of knockdown cells containing 4n DNA content), but likely because of an increase in multinuclear cells (Fig. 1G, vii and Fig. S34), although some of these 4n cells could be arrested in G2.

The multinuclear cells are likely the result of an improper cytokinesis, as there were numerous signs of incorrect mitotic divisions, with many cells displaying DNA bridges connecting daughter cells (Fig. 1G, vi and Fig. S34). Finally, in some cases we noticed a more severe cytokinesis phenotype, with one daughter cell containing the complete DNA content, whereas the other was completely devoid of chromatin (Fig. 1G, viii).

In addition to multinuclear cells, we also observed significant chromosome abnormalities in mitotic cells. Metaphase cells showed either a mass of under-condensed chromatin that was scattered along the spindle (Fig. 1G, iii) or condensed chromosomes that did not correctly congress to the metaphase plate (Fig. 1G, v). A very low number of anaphases were observed, but those that were present showed multiple lagging chromosomes and chromosome bridges (Fig. 1G, iv). No major defects were observed in the spindle, although some were longer and appeared to have a lower number of microtubules (Fig. 1G, iii). These phenotypes were specific to Gwl knockdown, as similar phenotypes were observed with two other siRNAs targeting different regions of hGwl mRNA (Fig. S3 B and C).

The mitotic defects observed after hGwl knockdown are indicative of a premature exit from mitosis. To assess whether this was the case, time-lapse movies were performed on synchronized HeLa cells stably expressing EB3-GFP and H2B-CherryFP. Scramble siRNA-treated cells progressed through mitosis normally (Fig. 2A and Movie S1). One of the major phenotypes observed at a 50-nM dose of hGwl siRNA was a decrease in the total number of cells that were able to perform mitosis during the experiment (65 vs. 80% in controls), suggesting that some cells were arrested at G2, similar to what has been described in *Xenopus* egg extracts (11). However, most cells were still able to enter into mitosis, albeit with numerous mitotic defects. Although the mitotic spindle structure did not contain any observable defects, in some cases the spindle rotated dynamically within the cell, performing several rotations (Fig. 2A, Fig. S4, and Movie S2). Moreover, some knockdown cells showed normal formation of the metaphase plate; however, chromosomes segregated incorrectly, resulting in the formation of DNA bridges (“segregation defects”) (Fig. 2A and Movie S3). Other cells displayed clear defects in chromosome congression, showing a high number of lagging chromosomes that were constantly present at the spindle poles and never correctly congressed to the metaphase plate. Many of these cells arrested during metaphase for long periods and finally died (“metaphase arrest”) (Fig. 2A and Movie S3), whereas others first delayed during metaphase and subsequently performed an aberrant anaphase, with significant chromosome segregation and cytokinesis defects (“metaphase delay”) (Fig. 2A and Movie S4). This delay or arrest in metaphase appeared to be mediated by the spindle assembly checkpoint (SAC), as the SAC proteins BubR1 and Aurora B were clearly localized at the kinetochores in hGwl-depleted cells (Fig. 2B). Finally, a subpopulation of cells displayed the most severe mitotic phenotype, in which cells entered and exited mitosis prematurely without forming a metaphase plate and with severe chromosome segregation defects (“no metaphase”) (Fig. 2A and Movie S5). In these cells, a cytokinesis furrow was formed and attempted to pinch through the DNA (Fig. S5), promoting the formation of multiple DNA bridges that were resolved by the cell rejoining and the formation of a multinuclear cell (Fig. 2A and Movie S5).

Comparing the different phenotypes (segregation defects, metaphase arrest, metaphase delay, and no metaphase) against the time spent in mitosis, we noticed that all hGwl knockdown cells had an increased transit time through mitosis. Mitotic length in the metaphase arrest and metaphase delay phenotypes was four times

longer compared with those of control cells. However, mitotic length in the segregation defects and no metaphase plate phenotypes was only twice that of controls (Fig. 2C), suggesting that despite the total absence of chromosome alignment, cells displaying a no metaphase plate phenotype were unable to maintain the mitotic state. No difference was observed in spindle rotation between the various subpopulation of hGwl-depleted cells, although cells that maintained prolonged SAC activity were more likely to rotate. Thus, similar to *Xenopus* extracts, one of the major phenotypes of hGwl knockdown is a premature exit from mitosis. The knockdown of hGwl at a 50-nM dose induced a variety of phenotypes, probably because of the intrinsic heterogeneity of the siRNA transfection procedure. To try to separate the various phenotypes, we repeated the experiment using various concentrations of hGwl siRNA (25, 50, and 100 nM). As the concentration of siRNA increased, there was a shift from cells that maintained the mitotic state (cells displaying the phenotypes segregation defects, metaphase arrest, and metaphase delay) toward cells incapable of maintaining mitosis (cells displaying the no metaphase plate phenotype) (Fig. 3A). Accordingly, mitotic length decreased concomitantly with the increasing siRNA concentration (Fig. 3B).

Furthermore, as the dose of siRNA increased, there was a significant delay in the time of mitotic entry (Fig. 3C), suggesting that cells were arrested in G2. To assess this issue in more detail,

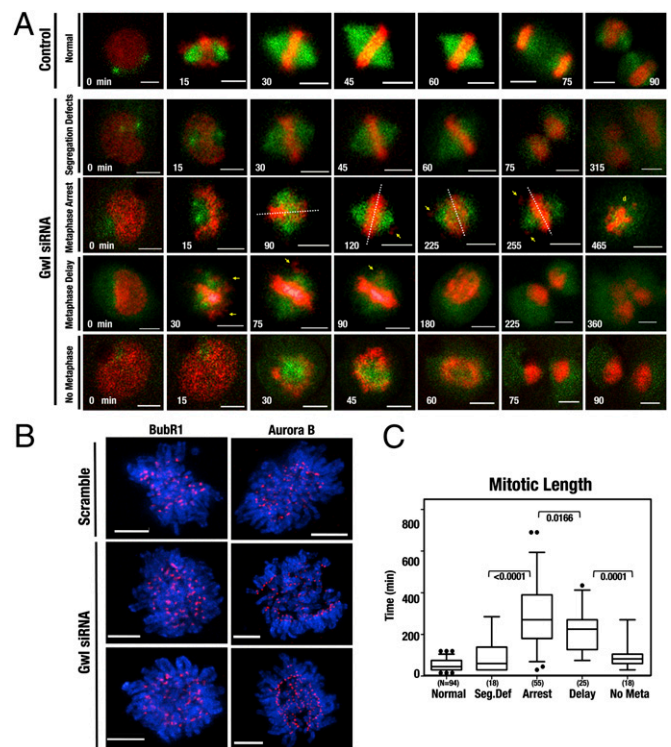
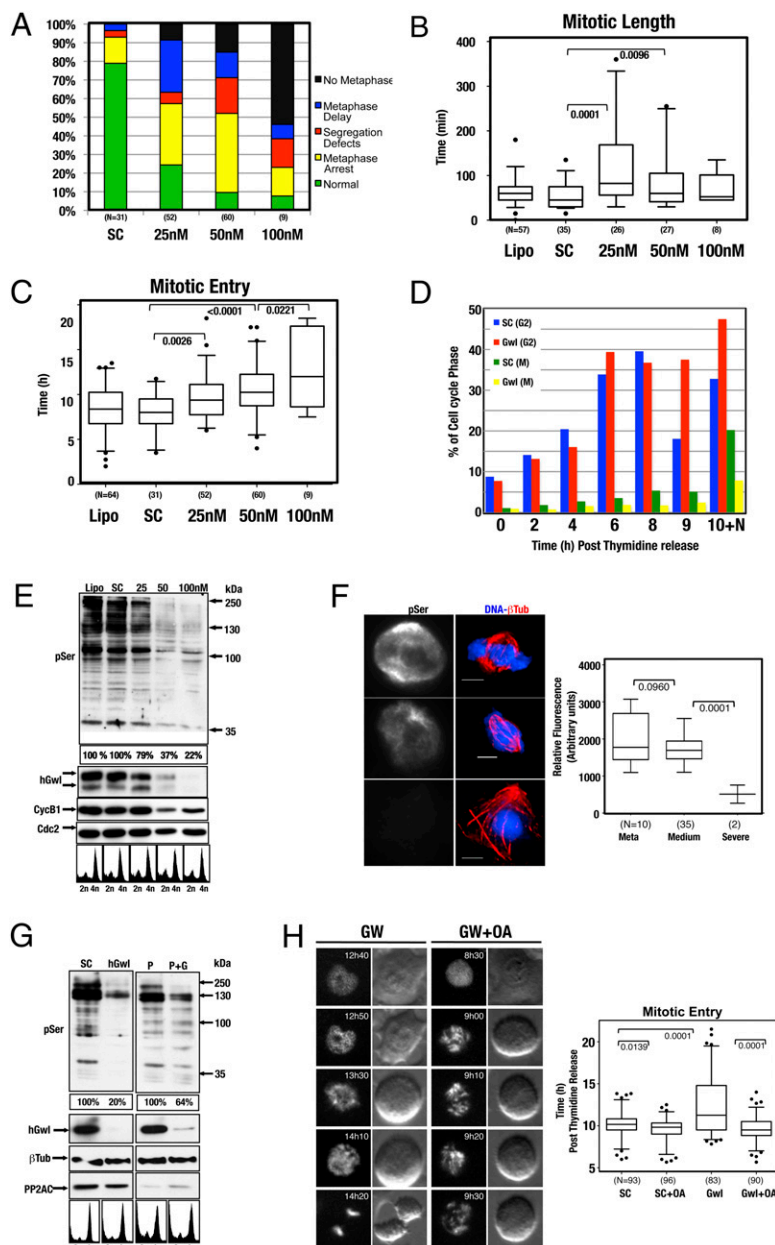


**Fig. 2.** hGwl knockdown promotes heterogeneity of phenotypes of varying severity in human cells. (A) HeLa cells stably expressing EB3-GFP (green) and H2B-CherryFP (red) were transfected with 50 nM of Scramble (Control) or hGwl siRNA for 24 h. After transfection, cells were synchronized with thymidine block. Movies were started 5 h after release and images were taken every 15 min. Notations indicate, time of the frame in minutes (white), lagging chromosomes (yellow arrows), metaphase plate orientation (dotted white lines), and cell death (yellow “d”). (Scale bars, 5  $\mu$ m.) (B) Mitotic HeLa cells were treated with scramble or hGwl siRNA and stained with anti-Aurora B or anti-BubR1 (red) antibodies and with DAPI (DNA, blue). Shown are the deconvoluted maximum projections from 0.3- $\mu$ m Z-sections. (Scale bars, 5  $\mu$ m.) (C) Cells from A were separated according to their mitotic phenotype and plotted against mitotic length. Mitotic entry was determined by analyzing the first signs of DNA condensation cross-reinforced with cell rounding. Mitotic exit was scored based on chromosome segregation at anaphase or DNA decondensation. Shown are box-plots with 5 to 95% confidence intervals (black dots indicate outliers). Two-tailed unpaired Student *t* tests were performed to determine statistical relevance; significant *P* values are shown.

**Fig. 3.** hGwl knockdown phenotypes can be rescued by the inactivation of PP2A. (A) Cells treated with increasing doses of hGwl siRNA were analyzed by time-lapse microscopy, as in Fig. 2A. The mitotic population was then scored on different criteria: cells that performed a correct mitosis (normal) and cells that displayed the various aberrant phenotypes (no metaphase plate, metaphase arrest, metaphase delay, and segregation defects). (B) Shown are box-plots for the mitotic length in non-transfected cells (Lipo) and cells transfected with Scramble siRNA (SC) or increasing doses of hGwl siRNA (25, 50, and 100 nM). Mitotic entry and exit was determined as in Fig. 2. The small percentage of siRNA-treated cells that completed mitosis correctly was not included in the analysis, as these were likely to be untransfected cells. The total number of cells observed in each condition is listed (N). Black dots indicate outliers. (C) Similar to B except that the time of mitotic entry instead of the mitotic length was measured. (D) HeLa cells were transfected with 100 nM of siRNA and synchronized with thymidine. The number of cells at S, G<sub>2</sub>, and mitosis at the indicated times was measured by 2D-FACS (propidium iodide versus anti-phospho Ser Cdk1 staining). In one instance, cells were released and treated with nocodazole (100 ng/mL) for 10 h to capture the mitotic population (10+N). (E) HeLa cells were transfected or not (Lipo) with scramble (SC) or increasing amounts of siRNA (25, 50, and 100 nM), synchronized by thymidine, and released into nocodazole (100 ng/mL) for 16 h. The phosphorylation of the different cyclin B-Cdc2 substrates (pSer), as well as the levels of cyclin B1, hGwl, and Cdc2 were analyzed. The pSer staining was equalized against Cdc2 and the percentage of staining in each condition is indicated. (F) HeLa cells were transfected with 50 nM of siRNA, synchronized by thymidine, and 16 h later analyzed by immunofluorescence using anti- $\beta$ -tubulin (red), anti-phospho Ser antibodies, and DAPI for DNA (blue). Cells were separated into the various mitotic phenotypes observed: normal metaphase (Meta), metaphase with uncongressed chromosomes or undercondensed chromatin scattered along the spindle (Medium), or cells that underwent mitotic exit (Severe). Identical acquisition exposure-time conditions were used to capture images. Scale bar, 5  $\mu$ m. The intensity of staining obtained with anti-phospho Ser antibody was measured in each unaltered cell and displayed as box-plots with 5 to 95% confidence intervals. Two-tailed unpaired student *t* tests were performed to determine statistical relevance; significant *P* values are shown. (G) HeLa cells were transfected with 100 nM of human Greatwall (hGwl), PP2AC (P), or both human Greatwall and PP2AC (P + G) siRNAs. The pSer was equalized against  $\beta$ -tubulin. Percentage of phosphorylation of the single hGwl knockdown (hGwl) was compared with scramble siRNA knockdown (SC), whereas the percentage of phosphorylation of the double PP2AC/hGwl knockdown (P + G) was compared with single PP2AC knockdown (P). FACS analysis confirmed that the majority of cells were arrested in G<sub>2</sub>/M. (H) HeLa H2B-CherryFP cells were transfected with 100 nM of Scramble (SC) or hGwl siRNA (GW) and, 24 h later, synchronized with thymidine. Six hours after release, cells were treated (+ OA) or not (SC and Gwl) with 500 nM of OA and followed by time-lapse microscopy with images captured every 10 min. Time of mitotic entry was determined by DNA condensation and cell detachment in each cell and displayed as box-plots with 5 to 95% confidence intervals. Two-tailed unpaired student *t* tests were performed to determine statistical relevance; significant *P* values are shown.



synchronized cells were analyzed by 2D FACS (Fig. 3D). Both Scramble- and hGwl siRNA-treated cells transited S and entered G<sub>2</sub> phase with similar kinetics, indicating that hGwl is not critical for S-phase progression. Entry into mitosis in Scramble cells began at 8 h, peaking at 9 h after thymidine release. In contrast, there was a clear impairment in the ability of hGwl-depleted cells to enter mitosis, with almost three times more (7.8 vs. 20.9%) mitotic cells present in the Scramble-treated nocodazole captured 10 h time-point (10+N). Thus, at the highest dose of hGwl siRNA, cells arrest in G<sub>2</sub>.

It has been recently shown that the inhibition of PP2A phosphatase activity is required to allow the phosphorylation of cyclin B-Cdc2 substrates, which promotes entry and maintains mitosis (3, 10, 11). Therefore, we next analyzed the capacity of these cells to phosphorylate the different cyclin B-Cdc2 substrates at the different doses of siRNA (Fig. 3E). As most cells

treated with a dose of 25 nM of siRNA arrest in mitosis after nocodazole treatment, we only observed a slight decrease in the levels of phosphorylation of cyclin B-Cdc2 substrates. However, at the higher doses of 50 and 100 nM, the phosphorylation levels of cyclin B-Cdc2 substrates were significantly reduced. These data are most likely a result of the G<sub>2</sub> arrest, although a partial degradation of cyclin B was also observed, probably as a result of cells that entered and subsequently slipped out of mitosis. In agreement with these results, we observed only a slight decrease in the immunostaining of cyclin B-Cdc2 substrates in mitotic hGwl-depleted cells (Fig. 3F), whereas a significant decrease in this signal was observed when cells prematurely exited mitosis (note decondensed DNA in the presence of a mitotic spindle). This decrease in the phosphorylation pattern of cyclin B-Cdc2 substrates was specific to hGwl knockdown, as it was mostly

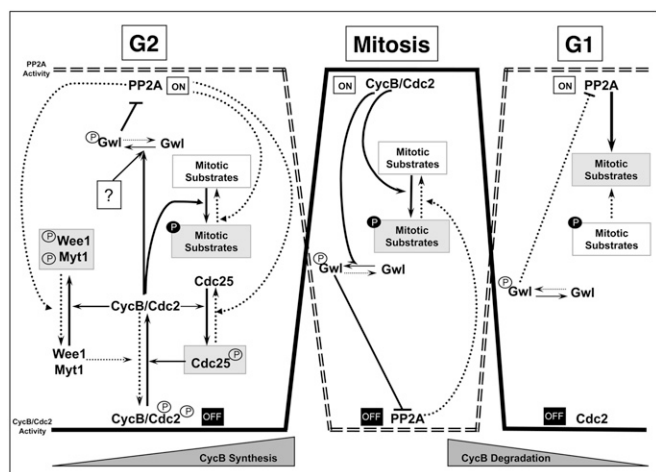


**Fig. 4.** Hypothetical model showing the different steps required for mitotic entry. Black arrows denote pathways active during mitotic entry. Dotted arrow denotes pathways that are inhibited at mitotic entry, during mitosis, or at mitotic exit.

rescued by the concomitant transfection of a siRNA-resistant plasmid encoding *Xenopus* Gwl (Fig. S6).

To assess if the decrease in cyclin B-Cdc2 substrate phosphorylation after hGwl knockdown could be the consequence of an increase in PP2A activity because of a loss of hGwl, we performed a double hGwl-PP2A siRNA knockdown (Fig. 3G). As expected, hGwl knockdown decreased the cyclin B-Cdc2 substrate phosphorylation by 80% in nocodazole captured cells. When PP2A siRNA knockdown was performed, we noticed that the general substrate phosphorylation pattern was partially decreased compared with the Scramble siRNA. This decrease is probably because of the 15% increase in cell death induced by PP2A depletion. Importantly, the double hGwl/PP2A knockdown rescued the general phosphorylation pattern of cyclin B-Cdc2 substrates from 20 to 64%. These results indicate that the hGwl knockdown phenotype is likely mediated by increased PP2A activity. However, it is possible that the knockdown of PP2A could promote a pleiotropic effect in other phases of the cell cycle (14). Thus, to more specifically investigate the role of Gwl in the regulation of PP2A activity at mitotic entry, we analyzed if the inhibition of this phosphatase by okadaic acid (OA) could rescue the G2 arrest, the most severe phenotype observed in hGwl knockdown cells. Cells transfected with 100 nM of hGwl siRNA, were synchronized in G1/S phase, treated with OA, and followed by time-lapse microscopy. The addition of OA at the end of S phase promoted a small but consistent advance in mitotic entry in Scramble- (SC) transfected cells (SC cells entered at an average time of 10 h 20 min after release versus 9 h 35 min in OA-treated cells) (Fig. 3H). As previously observed, hGwl knockdown cells delayed or arrested for a significant time in G2 (mean time of mitotic entry 12 h 12 min, with significant number of cells arrested in G2 for as long as 20 h postrelease) (Movie S6). Importantly, OA treatment rescued the G2 delay/arrest induced by hGwl knockdown and cells entered into mitosis with similar kinetics as control cells (mean-time of mitotic entry 9 h 45 min versus 9 h 35 min in OA-treated SC control cells), indicating that G2 arrest was mediated by an increased PP2A activity (Movie S7).

## Discussion

Historically, mitotic entry and exit was thought to be directly equivalent to cyclin B-Cdc2 activation and inactivation, respectively, and the activity of the phosphatases required for cyclin B/Cdc2 substrate dephosphorylation during mitosis was thought to be constant. According to this hypothesis, the large increase in cyclin B/cdc2 activity was sufficient to overcome the background dephosphorylation of mitotic substrates, thereby promoting mitotic entry. Similarly, inactivation of the cyclin B-Cdc2 complex by cyclin B degradation was sufficient to trigger mitotic exit. How-

ever, recent data from our and other laboratories has demonstrated that PP2A is highly regulated during mitotic entry and exit (3, 10, 11). Therefore, the old cell-cycle model now must be updated to include a different regulator of mitosis that modulates PP2A during this phase of the cell cycle. In this work we demonstrate that Gwl is this critical and evolutionally conserved regulator of PP2A in human cells.

Greatwall is a unique kinase whose role is essential in *Xenopus* egg extracts to promote mitotic entry and to maintain the mitotic state (8, 10, 11). Here, we identified MAST-L as the functional human ortholog of Gwl and demonstrated that its role is evolutionary conserved from *Xenopus* to human cells. During mitotic division, there is a highly regulated balance between cyclin B-Cdc2 and PP2A, and this balance dictates the phosphorylation level of mitotic substrates. The regulation of this balance, performed by Gwl-dependent inhibition of PP2A, is essential to allow the correct entry into and exit from mitosis. Accordingly, the phenotypes observed after hGwl knockdown likely reflect the differential phosphorylation pattern of cyclin B-Cdc2 substrates. Thus, cells lacking hGwl have a fully active PP2A that will completely dephosphorylate cyclin B-Cdc2 substrates, preventing cells from entering mitosis. Cells in which hGwl is partially present show an incomplete inactivation of PP2A. If this inactivation is sufficient, then cells can enter into mitosis, but display only a partial phosphorylation of the different mitotic substrates of cyclin B-Cdc2. Depending on the level of cyclin B-Cdc2-substrate phosphorylation, cells will display different mitotic defects, such as improper chromosome congression or spindle rotation, which in some cases leads to a permanent prometaphase arrest by the SAC, and in others can lead to mitotic slippage. In this regard, other reports described the presence of similar mitotic defects because of a partial inhibition of cyclin-Cdk activity (15–17). For example, siRNA knockdown of cyclin A results in improper chromosome congression and spindle rotation (15). Moreover, the inhibition of cyclin B-Cdc2 activity in mitotic cells also induced mitotic slippage, resulting in severe cytokinesis defects (17–19).

The exact mechanism of how Gwl regulates PP2A activity is currently unknown, although we previously demonstrated that xGwl can bind with PP2A/A and A/C (11). PP2A itself is a complicated ternary complex comprised of a catalytic subunit (C), a scaffold subunit (subunit A), and a regulatory B subunit (14). The substrate specificity of the PP2A complex is thought to be conferred by the B subunit that includes the B55 (B), B56 (B'), and B72/130 (B''), with each also containing multiple isoforms. Recently, PP2A-B55 $\delta$  was identified as a key phosphatase responsible for removing cyclin B/cdc2 phosphorylations (3). There are several possible phosphorylation sites in B55 $\delta$ , suggesting that this complex could be regulated by phosphorylation, perhaps by Gwl itself.

It is clear from our work and others that the classic cyclin/cdk cell-cycle model, must be perfectly coordinated with the phosphatases (especially PP2A) for correct mitotic entry, progression, and exit. In this regard, it has been shown that cyclin B-Cdc2 is capable of phosphorylating and activating Gwl kinase in vitro (8), suggesting that cyclin B-Cdc2 itself would induce PP2A inhibition through Gwl activation (Fig. 4). Thus, it is possible that at mitotic entry, cyclin B-Cdc2 is first activated and this activation would further induce Gwl phosphorylation and activation. Accordingly, our data identified a pool of Gwl localized at the centrosome during G2 phase, the same subcellular and temporal localization where cyclin B-Cdc2 is first activated (20). Activated Gwl could subsequently induce PP2A inhibition, permitting the correct phosphorylation of the different cyclin B-Cdc2 substrates. However, PP2A can also regulate cyclin B-Cdc2 activity, as the Wee1/Myt1 inhibitory kinases and the Cdc25 activatory phosphatase are themselves substrates of PP2A. Thus, the G2 arrest and the premature mitotic exit observed in Gwl knockdown cells are probably the result of both a dephosphorylation of cyclin B-Cdc2 substrates and a subsequent inhibition of cyclin B-Cdc2 by Myt1/Wee1/Cdc25 dephosphorylation. Therefore, cyclin B-Cdc2 kinase cannot be activated at mitotic entry if there is not at first a partial inhibition of PP2A. This inhibition of PP2A could be mediated by a partial activation of Gwl through a cyclin B-Cdc2-independent phosphorylation of Gwl. Once cyclin B-Cdc2 is activated, it could act as the starter, promoting full activation of Gwl and mitotic phosphorylation. The fact that cyclin B-Cdc2 could be one of the starters that promotes mitotic entry

would assure that cells enter into mitosis only when a complete activation of this kinase is achieved.

Once cells enter into mitosis, Gwl-dependent inhibition of PP2A is still required to maintain the mitotic state. We have previously demonstrated that even in the presence of a high cyclin B-Cdc2 activity, the substrates of this kinase become dephosphorylated and *Xenopus* egg extracts slip out of mitosis when PP2A cannot be inactivated by Gwl (11). Finally, at mitotic exit, cyclin B is degraded by the ubiquitin-dependent pathway, promoting the inactivation of the cyclin B-Cdc2 complex. This inactivation results in the dephosphorylation of Gwl and the reactivation of PP2A. Once activated, PP2A induces dephosphorylation of mitotic substrates, triggering an irreversible exit from mitosis until the next G<sub>2</sub>, when cyclin B will accumulate again. Interestingly, to date, mitotic slippage has been solely attributed to the slow continual degradation of cyclin B (21). However, from our results, premature activation of PP2A or loss of Gwl during mitosis is a unique mechanism that could induce mitotic slippage independently of cyclin B degradation. This finding could have broad implications in defining new chemotherapies for cancer treatments that target the mitotic slippage pathway.

## Materials and Methods

**Chemicals, Reagents, and Antibodies.** MG132 and OA were purchased from Calbiochem. Anti-Cyclin B1 and Cdc2 (Santa Cruz), anti-Phospho-(Ser) CDK Substrate and Phospho-Cdc2-Tyr15 (Cell Signaling), monoclonal 1D6 against PP2AC (Millipore), anti-Aurora B and BUBR1 (Becton Dickinson), and monoclonal anti- $\gamma$  and  $\beta$ -Tubulin (Sigma-Aldrich) were used. Anti-Cdc25 and Cdc27 were obtained as previously described (7, 19–22). pCMVSPORT6-MAST-L was obtained from RZPD Deutsches Ressourcenzentrum fuer Genomforschung GmbH, amplified by PCR and subcloned in the pGEX4T2 plasmid. The fusion protein was expressed in *Escherichia coli*. Inclusion bodies were prepared and used to immunize rabbits. Immune serum against the full-length protein (anti-hGwl) was affinity-purified on an immobilized GST-MAST-L column. Anti-C-terminal hGwl antibodies were also generated against the last 12 amino acids of the C-terminal sequence of this protein. Peptides were coupled to thyroglobulin for immunization and to immobilized BSA for affinity purification, as previously described (23).

**Cell Synchrony.** Thymidine block/release synchronizations were performed as previously described (24). For nocodazole synchrony, cells were first released from G1/S thymidine block, and treated with 100 ng/mL of nocodazole for 16 h. Floating cells were then removed, washed three times, and seeded back in fresh media.

**siRNA Design and Transfection.** The Promega T7 Ribomax Express RNAi system was used to produce in vitro transcribed siRNAs against human Gwl and PP2Ac. The following target sequences were identified and appropriate sense

and antisense oligonucleotides were synthesized. For human Gwl positions from #1 = 389–409, #2 = 840–860, and #3 = 1516–1536. For PP2Ac, position #169–187, which targeted both  $\alpha$  and  $\beta$  isoforms. The following Scramble sequence was used SC = GGATTGTGCGGCATTAAC, as a control. Transfection of siRNA was performed using Lipofectamine RNAiMax Reagent (Invitrogen) as per the manufacturer's instructions. Rescue experiments were performed as per Fig. S6. Briefly, synchronized HeLa cells were first transfected with hGwl siRNA sequence #2 and subsequently transfected with a plasmid (PCS2) encoding full length *Xenopus* Gwl. Cells were synchronized, captured in mitosis with nocodazole, and analyzed by Western blot.

**Immunofluorescent Staining.** Cells were grown on poly-lysine coated glass coverslips and permeabilized for 30 s in PHEM buffer (60 mM Pipes, 25 mM hepes, 1 mM EGTA, 2 mM MgCl<sub>2</sub>) plus 0.25% Triton X-100. Then, cells were fixed for 10 min in PHEM buffer with 3.7% formaldehyde and 0.5% Triton X-100, washed, and blocked (3% BSA, 0.1% tween 20 in PBS) for 30 min. Primary antibodies were incubated for 2 h at room temperature in blocking solution. Images were captured using a Leica DM6000 microscope coupled with a Coolsnap HQ2 camera, using a Leica 63 $\times$  APO 1.4 lens, powered by metamorph 7.1 software. For mitotic cells, 0.3- $\mu$ m Z-sections were taken and deconvoluted using Huygens 3.0 software. Maximum projections and total fluorescence measurements were performed with Image J, metaphase plate measurements and false coloring were performed using Photoshop CS4 Extended software.

**Live Cell Imaging.** Thymidine-synchronized cells were filmed with a Micromax YHS 1300 camera coupled to a Zeiss Axiovert 200 M inverted microscope fitted with a Zeiss slider PlasDIC 32 $\times$  LD A plan NA 0.4 lens, Zeiss mercury lamp, and controlled by Metamorph 7.1 software (Molecular Devices). Images, both phase-contrast and GFP/CherryFP fluorescence, were taken every 10 to 15 min. The resulting images were processed, analyzed, and false-colored using Photoshop CS4 Extended software. Box graphs and statistical analysis was performed using GraphPad Prism 5. Mitotic entry, length, exit, and cell death were determined as described in Fig. S7. Briefly, the following parameters were used to identify mitotic entry: first appearance of a mitotic spindle with condensed chromosomes, loss of a nucleolus, and rounding up of the cell from the culture plate. Exit was scored based on the first appearance of anaphase, thus visualization of chromosome separation, pinching of the membrane, and appearance of a midbody.

**ACKNOWLEDGMENTS.** We thank Dr. J. Ellenberg (European Molecular Biology Laboratory) and Dr. V. Doye (Institut Jacques-Monod) for the generous gift of the HeLa EB3/H2B cell line, Montpellier RIO Imaging for microscopy facilities, and B. Gabrielli and K. Rogowski for helpful comments on the manuscript. This work was supported by the Ligue Nationale Contre le Cancer (Equipe Labellisée, 2004–2008). A.B. and E.B. are "Fondation pour la Recherche Medicale" and "Ligue Nationale Contre le Cancer" Fellows respectively.

- Jackman MR, Pines JN (1997) Cyclins and the G<sub>2</sub>/M transition. *Cancer Surv* 29:47–73.
- Bollen M, Gerlich DW, Lesage B (2009) Mitotic phosphatases: From entry guards to exit guides. *Trends Cell Biol* 19:531–541.
- Mochida S, Ikeo S, Gannon J, Hunt T (2009) Regulated activity of PP2A-B55 delta is crucial for controlling entry into and exit from mitosis in *Xenopus* egg extracts. *EMBO J* 28:2777–2785.
- Morgan DO (1997) Cyclin-dependent kinases: Engines, clocks, and microprocessors. *Annu Rev Cell Dev Biol* 13:261–291.
- Glotzer M, Murray AW, Kirschner MW (1991) Cyclin is degraded by the ubiquitin pathway. *Nature* 349:132–138.
- Bettencourt-Dias M, et al. (2004) Genome-wide survey of protein kinases required for cell cycle progression. *Nature* 432:980–987.
- Yu J, et al. (2004) Greatwall kinase: A nuclear protein required for proper chromosome condensation and mitotic progression in *Drosophila*. *J Cell Biol* 164:487–492.
- Yu J, Zhao Y, Li Z, Galas S, Goldberg ML (2006) Greatwall kinase participates in the Cdc2 autoregulatory loop in *Xenopus* egg extracts. *Mol Cell* 22:83–91.
- Zhao Y, et al. (2008) Roles of Greatwall kinase in the regulation of cdc25 phosphatase. *Mol Biol Cell* 19:1317–1327.
- Castilho PV, Williams BC, Mochida S, Zhao Y, Goldberg ML (2009) The M phase kinase Greatwall (Gwl) promotes inactivation of PP2A/B55delta, a phosphatase directed against CDK phosphatases. *Mol Biol Cell* 20:4777–4789.
- Vigneron S, et al. (2009) Greatwall maintains mitosis through regulation of PP2A. *EMBO J* 28:2786–2793.
- Gandhi MJ, Cummings CL, Drachman JG (2003) FLJ14813 missense mutation: A candidate for autosomal dominant thrombocytopenia on human chromosome 10. *Hum Hered* 55:66–70.
- Johnson HJ, et al. (2009) In vivo inactivation of MASTL kinase results in thrombocytopenia. *Exp Hematol* 37:901–908.
- Janssens V, Goris J (2001) Protein phosphatase 2A: A highly regulated family of serine/threonine phosphatases implicated in cell growth and signalling. *Biochem J* 353:417–439.
- Beamish H, et al. (2009) Cyclin A/cdk2 regulates adenomatous polyposis coli-dependent mitotic spindle anchoring. *J Biol Chem* 284:29015–29023.
- Burgess A, et al. (2006) Inhibition of S/G<sub>2</sub> phase CDK4 reduces mitotic fidelity. *J Biol Chem* 281:9987–9995.
- Potapova TA, et al. (2006) The reversibility of mitotic exit in vertebrate cells. *Nature* 440:954–958.
- Potapova TA, Daum JR, Byrd KS, Gorsky GJ (2009) Fine tuning the cell cycle: Activation of the Cdk1 inhibitory phosphorylation pathway during mitotic exit. *Mol Biol Cell* 20:1737–1748.
- Vassilev LT, et al. (2006) Selective small-molecule inhibitor reveals critical mitotic functions of human CDK1. *Proc Natl Acad Sci USA* 103:10660–10665.
- Jackman M, Lindon C, Nigg EA, Pines J (2003) Active cyclin B1-Cdk1 first appears on centrosomes in prophase. *Nat Cell Biol* 5:143–148.
- Brito DA, Rieder CL (2006) Mitotic checkpoint slippage in humans occurs via cyclin B destruction in the presence of an active checkpoint. *Curr Biol* 16:1194–1200.
- Lorca T, et al. (1998) Fizzy is required for activation of the APC/cyclosome in *Xenopus* egg extracts. *EMBO J* 17:3565–3575.
- Abrieu A, et al. (2001) Mps1 is a kinetochore-associated kinase essential for the vertebrate mitotic checkpoint. *Cell* 106:83–93.
- Gabrielli BG, De Souza CP, Tonks ID, Clark JM, Hayward NK, Ellem KA (1996) Cytoplasmic accumulation of cdc25B phosphatase in mitosis triggers centrosomal microtubule nucleation in HeLa cells. *J Cell Sci* 109:1081–1093.